2021 43rd Annual International Conference of the
IEEE Engineering in Medicine & Biology Society (EMBC)
Oct 31 - Nov 4, 2021. Virtual Conference

Channel Synergy-based Human-Robot Interface for a Lower Limb Walking Assistance Exoskeleton

Kecheng Shi[1,2,3], Rui Huang[1,2,3*], Fengjun Mu[2,3], Zhinan Peng[1,2,3], Jie Yin[4], Hong Cheng[1,2,3]

Abstract— **The human-robot interface (HRI) based on surface electromyography(sEMG) can realize the natural interaction between human and robot. It has been widely used in exoskeleton robots recently to help predict the wearer's movement. The sEMG signal of the paraplegic patients' lower limbs is weak. How to achieve accurate prediction of the lower limb movement of patients with paraplegia has always been the focus of attention in the field of HRI. Few studies have explored the possibility of using upper limb sEMG signals to predict lower limb movement. In addition, most HRIs do not consider the contribution and synergy of sEMG signal channels. This paper proposes a human-exoskeleton interface based on upper limb sEMG signals to predict lower limb movements of paraplegic patients. The interface constructs a channel synergy-based network (MCSNet) to extract the contribution and synergy of different feature channels. An sEMG data acquisition experiment is designed to verify the effectiveness of MCSNet. The experimental results show that our method has a good movement prediction performance in both within-subject and cross-subject situations, reaching an accuracy of** 94.51% **and** 80.75% **respectively.**

I. INTRODUCTION

The development of artificial intelligence technology and wearable sensors has promoted the rise of human-robot interaction. As the core of human-robot interaction, an HRI enables direct communication with a robot via physical or biological signals, which has received widespread attention in the past decade [1]. Exoskeleton is a typical application scenario of HRI, some HRI based on physical signals, such as inertial measurement units or pressure signals, have been used in the walking-assistant exoskeleton to realize the movement prediction of patients with hemiplegia/paraplegia [2-4]. In recent years, with the decoding of biological signals, HRI based on biological signals (such as electroencephalogram and electromyography) have been designed, opening up the possibility of realizing more natural and efficient movement predictions between human and exoskeleton [5-7]. For paraplegic patients, the loss of lower limb motor and sensory function makes the exoskeleton difficult to predict the patients' movement, and the previous work has not yet proposed a high-efficiency HRI specifically for paraplegic patients. Therefore, it is urgent to propose an HRI with high movement prediction accuracy for paraplegic patients.

Brain-computer interface (BCI) is an HRI based on electroencephalogram (EEG). It can directly obtain patients' motion intention from the EEG signal and without actual limb movement, so the BCI has been used to predict the movement of paraplegic patients [8-10]. But EEG signal's signal-to-noise ratio is low, it is susceptible to interference from the environment and the patient's own limb movement and mood, which is unacceptable for the exoskeleton movement assistance tasks of paraplegic patients.

Compared with the EEG signal, the sEMG signal has a higher signal-to-noise ratio and is less interfered with by external factors. Therefore, the sEMG-based human-robot interface (MHRI) has been earlier and more widely used in the walking-assistant exoskeleton [11, 12]. Given the weak sEMG signal of the paraplegic patients' lower limbs, recent studies have explored the possibility of predicting the lower limb movement based on the sEMG signal of the upper body [13]. Most of these methods simply use the manual extraction feature and machine learning classification models to predict the lower limb movements of the paraplegia, and the classification effect and the accuracy of the movement prediction are generally low.

Deep learning has largely alleviated the need for manual feature extraction, achieving state-of-the-art performance in fields such as computer vision and natural language processing [14, 15]. In fact, deep convolutional neural networks (CNNs) can automatically extract appropriate features from the data. It has succeeded in many challenging image classification tasks [16, 17], surpassing methods that rely on handcrafted features [14, 17]. Although most research still relies on handcrafted features, many recent works have explored the application of deep learning in MHRI [18-20]. This kind of MHRI mostly combines long short-term memory networks (LSTM) and CNNs simply, ignoring the difference in contribution and synergy of sEMG feature channels of different subjects under the same movement. Moreover, most researchers do not pay much attention to whether the features extracted by CNNs have physiological significance.

In this paper, a channel synergy-based human-exoskeleton interface is proposed for lower limb movement prediction in paraplegic patients. It uses the sEMG signals of 12 upper

[1]Kecheng Shi, Rui Huang, Zhinan Peng, Hong Cheng are with the School of Automation Engineering, University of Electronic Science and Technology of China, Chengdu, China.

[2]Kecheng Shi, Rui Huang, Zhinan Peng, Hong Cheng, Fengjun Mu are with the Engineering Research Center of Human Robot Hybrid Intelligent Technologies and Systems, Ministry of Education, University of Electronic Science and Technology of China, Chengdu, China.

[3]Kecheng Shi, Rui Huang, Zhinan Peng, Hong Cheng, Fengjun Mu are with the Center for Robotics, University of Electronic Science and Technology of China, Chengdu, China.

[4]Jie Yin is with the College of MedicineSouthwest Jiaotong University-ChengduChina.

*Rui Huang is the corresponding author. ruihuang@uestc.edu.cn

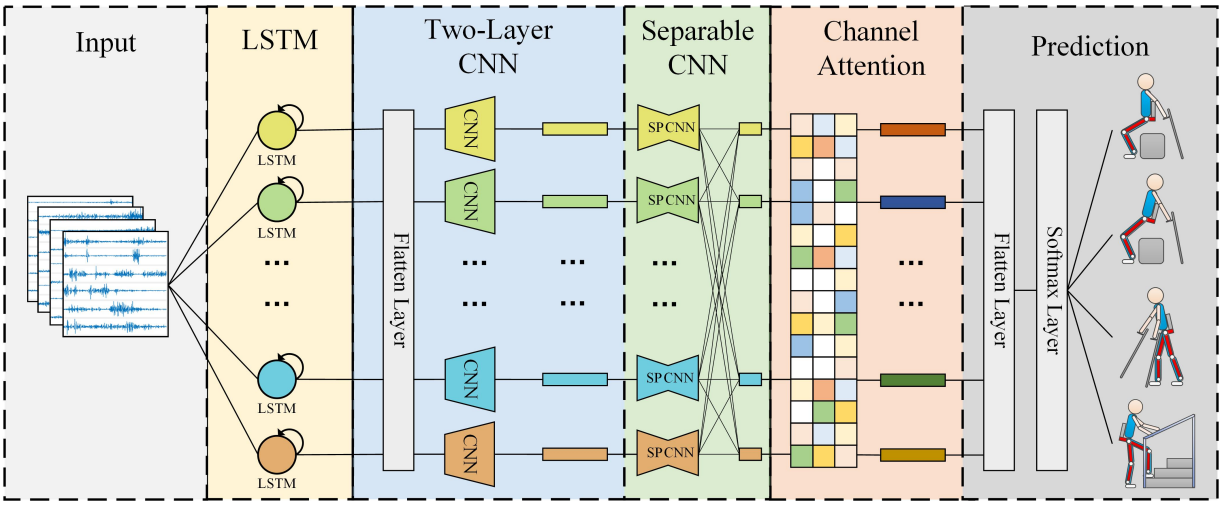

Fig. 1. Overall architecture of the MCSNet model. Lines denote the convolutional kernel connectivity between inputs and outputs (called feature maps). The network starts with a channel-by-channel LSTM (second column) to learn the timing feature, then uses a two-layer convolution (third column) to learn different spatiotemporal features. The separable convolution (fourth column) is a combination of a depthwise convolution followed by a pointwise convolution, which can explicitly decouple the relationship within and across feature maps and learns the synergy feature of sEMG.)

limb muscles to predict the lower limb movements. The proposed movement prediction model uses LSTM, depthwise and separable convolutions to extract the spatiotemporal features of multi-channel sEMG signals, and introduces an attention module to extract the synergy of different sEMG feature channels. An sEMG data acquisition experiment is designed to verify the proposed channel synergy-based network (MCSNet). The experimental results verify that MCSNet's prediction accuracy is better than the traditional machine learning-based MHRI and two mainstream deep learning-based MHRI in both within-subject and cross-subject situations.

II. METHOD

This section presents the methodology details of the proposed movement prediction model. Section II-A describes the overall architecture of the MCSNet model. In section II-B, we introduce seven traditional MHRIs and two mainstream deep learning-based MHRIs, which are used to compare to the MCSNet model.

A. Description of the MCSNet Model

Fig. 1 visualizes the proposed MCSNet model. The entire model architecture consists of three parts. The first part is data input, input the processed sEMG data; the second part is feature extraction, which mainly contains four blocks, each block establishes the connection between the feature channels of the sEMG signal in different dimensions; the third part is movement classification/prediction, which classifies the extracted features. This section mainly describes the feature extraction part, because it is the core of the entire model. For sEMG trials, it was collected at a 1500 Hz sampling rate, having C channels and T time samples.

- In block 1, for each input sEMG sample segment (size $C \times 300$, multiple shown in Figure 1), we performed a channel-by-channel LSTM step to extract the timing features of different signal channels. Since the deepening of the LSTM layers will cause over-fitting, we found this phenomenon is more serious for sEMG data during the experiment, so we choose to use a single-layer LSTM as the timing feature extraction block. In this process, we define the k-th sEMG channel signal as

$$F_{sEMG}^{k}, (k = 1, ..., C) \tag{1}$$

which k indicates the serial number of the channel. In order to better describe the relationship between the LSTM block and the sEMG feature channel, a more fine-grained channel-by-channel representation is used. The operation with LSTM block is defined as follows:

$$F_{temp}^{k} = N_{lstm}^{k}(F_{sEMG}^{k}), \tag{2}$$

In eq. (2), each of the sEMG signal channels is used to generate its timing feature independently, the timing feature from all the channels will be contacted into F_{temp}, which size is $C * L$, L represents the length of input signal's sample. Since the input feature channel $F_{sEMG}^{k}, (k = 1, ..., C/2)$ and $F_{sEMG}^{k+C/2}, (k = 1, ..., C/2)$ in our data acquisition process is opposite the left and right symmetrical relationships on the muscle blocks in the acquisition, the muscles of the symmetry position have similar behavior patterns when the subjects are under various movements, so we use the LSTM units with shared weights used in the corresponding channel.
- In block 2, we perform two convolutional steps in sequence. First, we fit F_1 2D convolution filters with a size of (1, 65) and output F_1 feature maps containing different timing information. We then use a depthwise convolution of size (C, 1) to extract spatial features for every channel. This operation provides a direct way to learn spatial filters for different timing information, which can effectively extract different timing and spatial

features. The depth parameter D represents the number of spatial filters to be learned for each time series feature map (D=1 is shown in Figure 1 for illustration purposes).In this block, F_{temp} is transformed with the first convolution layer as follows:

$$F_{conv} = N_{conv}(F_{temp}), \tag{3}$$

$$F_{d-conv} = N_{d-conv}(F_{conv}), \tag{4}$$

In eq. (3) and eq. (4), the size of F_{conv} and F_{d-conv} is $F_1 * C * L$ and $(D * F_1) * 1 * L$, respectively.

- In block 3, we use a separable convolution, a depthwise convolution of size (1, 15) followed by F_2 pointwise convolutions of size (1, 1). The separable convolutions first learn the kernel of each spatiotemporal feature map individually, then optimally merge the outputs afterward, which can explicitly decouple the relationship within and across feature maps. This operation separates the learning of spatiotemporal features from the combination of optimal features, which is very effective for sEMG signals. Because sEMG signals have different synergy between channels when performing different movements (muscle synergy effect [21]), this is similar to a synergy feature, which the separable convolutions can extract. Because the padding is used in the first stage of separable convolution, and the pixel-wised convolution will not change the size of the feature, the output $F_{sep-conv}$ has the same size as F_{d-conv}.
- For block 4, we introduced a channel attention module. This operation learns the weights of different synergy features, which can effectively associate movements with the most relevant synergy features and improve the movement prediction accuracy. Moreover, there are differences in the feature contributions of sEMG channels in different subjects under the same movement (muscle compensatory behavior [22]), which will amplify the differences in the synergy feature of different subjects under the same movement. The channel attention module can learn different weights for different subjects to deal with the differences in synergy features, thereby improving the robustness of the entire movement prediction model.

We input the generated attention-based spatiotemporal features into the movement classification/prediction part. As shown in fig. 1, the extracted features first perform a Flatten layer step, and then pass directly to a softmax classification with N units, where N is the number of classes in the data. The entire model architecture uses the cross-entropy loss function to optimize the parameters, and input 10 sEMG samples with time-sequence everytime.

B. Comparison with Other MHRI Movement Prediction Approaches

1) Comparison with Traditional MHRI Movement Prediction Approaches: We compared the performance of MCSNet with seven traditional MHRI based on handcrafted features and machine learning models in lower limb movement prediction. In the selection of features, referring to the research conclusions of time domain and frequency domain features in the literature [23] and four commonly used feature sets [24, 25], we finally select the feature of Mean Absolute Value (MAV), WaveLength (WL), Zero Crossings (ZC), 6-order AutoRegressive coefficient (6-AR), and average Power Spectral Density (PSD). Furthermore, we choose Linear Discriminant Analysis (LDA), Decision Tree (DT), Naive Bayes (BES), Linear Kernel-based Support Vector Machine (LSVM), Radial Basis Function-based Support Vector Machine (RBFSVM), K Nearest Neighbor (KNN), and Artificial Neural Network (ANN) as the classification/prediction model. We use MATLAB's Classification Learner Toolbox and Neural Net Pattern Recognition Toolbox to implement these models.

2) Comparison with Deep Learning-based MHRI Movement Prediction Approaches: In deep learning, we compared the performance of MCSNet with two layer CNN and CNN-LSTM models. The two layer CNN architecture consists of two convolutional layers and a softmax layer which is for classification. The CNN-LSTM architecture includes two LSTM layers, three convolutional layers, and a softmax layer. We implemented these models in PyTorch. For specific details of the model, see `https://github.com/mufengjun260/MCSHRI`.

III. EXPERIMENTS AND RESULTS

In this part, an sEMG signal acquisition experiment based on upper limb muscles is designed to verify the effectiveness of the method proposed in this paper. Section III-A describes the process of the acquisition experiment and the process of data preprocessing. Section III-B gives the implementation details of model training. In Section III-C, we show the MCSNet movement prediction model results and compare MCSNet with other movement prediction models in the case of within-subject and cross-subject.

A. sEMG Data Acquisition Experiment

A total of 8 healthy subjects were invited to participate in the experiment. Each subject completed four lower limb movements of standing, sitting, walking and going up stairs while wearing the AIDER exoskeleton. During this period, the sEMG signals of the subjects' upper limbs were collected.

1) ***Participants***: The eight subjects (7 males, one female) had an average age of 26 years, a height between $165-185$ *cm*, and a weight between $59-82$ *kg*. All subjects can independently use the AIDER exoskeleton to complete the lower limb movements involved in the experiment, and are in good physical condition with no injuries to the arm. Before the experiment, each subject had been explained the contents of the experiment and signed an informed consent form. This experiment was approved by the Research Ethics Committee of the University of Electronic Science and Technology of China.

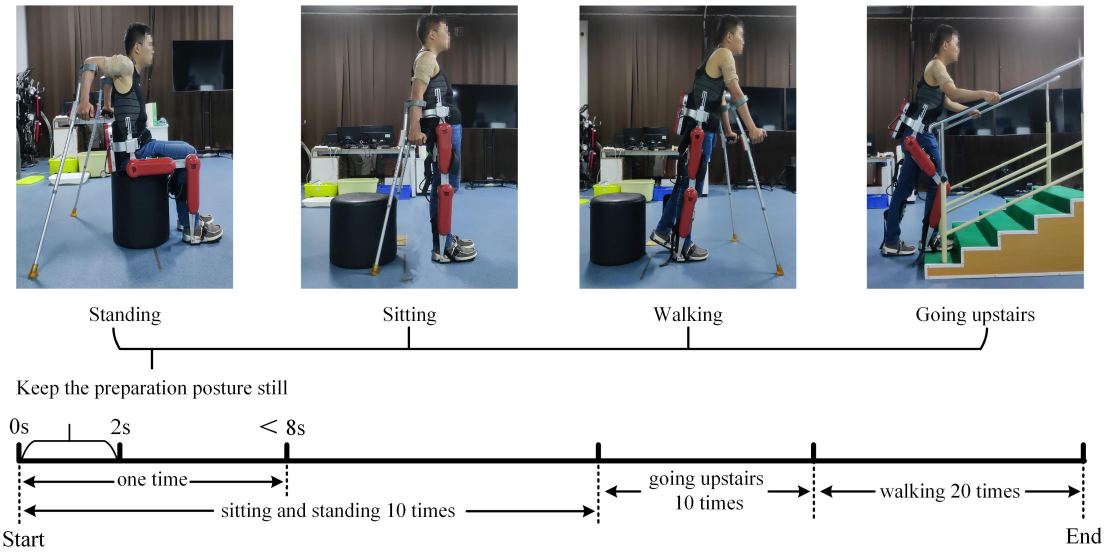

Fig. 2. Schematic diagram of sEMG data acquisition experiment. The upper part is the preparation posture of the four lower limb movements, We fixed the sEMG acquisition electrode with an elastic bandage to prevent the acquisition electrode from falling off during the experiment. The lower part is the schematic diagram of the experimental acquisition process.)

2) ***Procedures***: Before the experiment, record the relevant physical parameters of the subject, inform the experimental procedure to the subject, and let the subject use crutches to freely practice the four lower limbs movements of standing, sitting, walking, and going upstairs while wearing the AIDER exoskeleton for 30 *min*. Then paste sEMG acquisition electrodes on the 12 muscles of the subject's left and right upper limbs, including the deltoid anterior, biceps, and superior trapezius muscles (as shown in fig. 3). The subject puts on the AIDER exoskeleton, supports the crutches with both hands, stands in the designated position, and completes the sitting, standing, and going upstairs movements 10 times after hearing the instructions, and then completes walking movement 20 times (a complete gait cycle is one time). Each movement is completed within 8 seconds, all subjects are required to perform the specified movements without using their legs as much as possible to ensure that the collected upper limb sEMG signals are close to the paraplegic patients. After the movement starts, the subject maintains the lower limb movement preparation posture for 2 *sec* (see fig. 2) and then controls the AIDER exoskeleton to complete the corresponding lower limb movement. Throughout the experiment, the camera is turned on to record, and myoMUSCLE (an sEMG acquisition device, Scottsdale, American) is used to collect the sEMG signals of the upper limbs.
3) ***Data Processing***: myoMUSCLE (1500 Hz) collects the upper limb sEMG signal data of each lower limb movement of the subject throughout the whole process. After obtaining the sEMG data, a 50 Hz notch filter is used to remove the power frequency interference of the current, and a 10-450 Hz bandpass filter is used to retain the effective information of the sEMG signal. Since our application is lower limb movement prediction, we only intercept the sEMG data during the movement preparation period (the period when keeping the preparation posture still).In addition, to achieve continuous movement prediction of lower limb, this paper uses 200 *ms* (including 300-time series data) as a time window to segment the sEMG signal, and the movement step of the time window is 100-time series data.

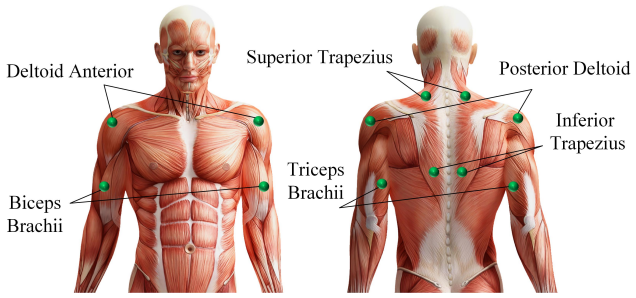

Fig. 3. The upper limb muscle used in sEMG data acquisition experiment.

B. Implementation Details

MCSNet and the deep learning-based MHRI movement prediction models are implemented using the PyTorch library [25]. In MCSNet, both LSTM's output and hidden unit are of dimension 300, and the network's hyper-parameters (D, F_1, L) is set to (2, 12, 300). Exponential linear units(ELU) [26] are used to introduce the nonlinearity of each convolutional layer. To train ours and other deep learning-based models, we use the Adam optimizer to optimize the model's parameters, with default setting described in [27] to minimize the categorical cross-entropy loss function. We run 1000 training

TABLE I

WITHIN-SUBJECT MOVEMENT PREDICTION PERFORMANCE (TEST SET ACC).

	Traditional Machine Learning-based MHRI							Deep Learning-based MHRI		
Subject	**LDA**	**DT**	**BES**	**LSVM**	**RBFSVM**	**KNN**	**ANN**	**TCNN**	**CNN-LSTM**	**MCSNet**
1	0.9200	0.7520	0.8496	0.9451	0.9504	0.8387	0.9315	0.8377	0.9570	**0.9928**
2	0.8731	0.8097	0.7718	0.9026	0.9159	0.8000	0.9008	0.5849	0.9034	**0.9295**
3	0.7105	0.8724	0.7852	0.8146	0.8503	0.6018	0.7590	0.7722	0.9089	**0.9772**
4	0.7888	0.6630	0.6818	0.8594	0.8526	0.7294	0.8428	0.7543	0.9075	**0.9513**
5	0.7430	0.7962	0.4937	0.8675	0.8911	0.7091	0.8828	0.8525	**0.9434**	0.9212
6	0.8872	0.8188	0.6747	**0.8936**	0.8927	0.8358	0.8923	0.8373	0.8844	0.8437
7	0.9600	0.8467	0.7263	0.9602	0.9687	0.8261	0.9523	0.7576	0.9960	**1.0000**
Average ACC	0.8404	0.7941	0.7119	0.8918	0.9031	0.7630	0.8802	0.7709	0.9287	**0.9451**

iterations (epochs) and perform validation stopping, saving the model weights, which produce the lowest validation set loss. All models are trained on NVIDIA RTX2080Ti, with CUDA10.1 and cuDNN V7.6. Our code implementation can be found in `https://github.com/mufengjun260/MCSHRI`.

C. Experiments Result

We compared the performance of the proposed MCSNet model with other MHRIs in movement classification/prediction in both the within-subject and cross-subject situations.

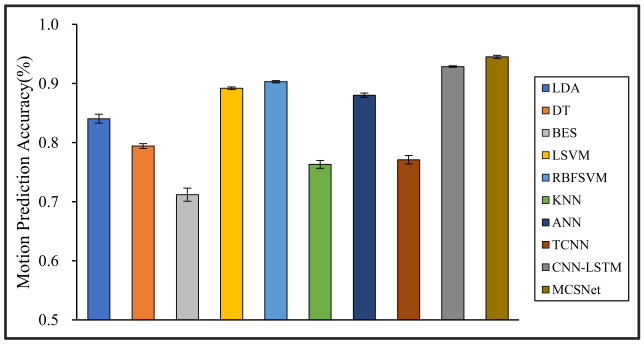

Fig. 4. Within-subject movement prediction performance, four-fold cross-validation is used to avoid the phenomenon of model overfitting, averaged over all folds and all subjects. Error bars denote two standard errors of the mean.

1) Within-Subject Classification: For within-subject, we divide the data of the same subject according to a ratio of 7:3 and then use 70% of the data to train the model for that subject. We compare the performance of both traditional machine learning-based MHRI movement prediction models (LDA, DT, BES, LSVM, RBFSVM, KNN, and ANN) and deep learning-based MHRI movement prediction models (TCNN and CNN-LSTM) with MCSNet. Within-subject results across all models are shown in Figure 4. It can be observed, across the average lower limb movement prediction accuracy of 7 subjects, MCSNet outperforms traditional machine learning-based and deep learning-based MHRI models. But there is no significant statistical difference ($P > 0.05$). Among the traditional MHRI movement prediction models, the RBFSVM model has the highest average accuracy of 7 subjects, reaching 90.31%. It is consistent with the conclusions obtained in previous work [28]. Table I shows the prediction accuracy of each subject under different MHRI movement prediction models. It can be found that the same movement prediction model has a large difference in the accuracy for different subjects (especially the traditional MHRI movement prediction model). In contrast, MCSNet has a high accuracy rate of lower limb movement prediction for all subjects, and the accuracy rate is evenly distributed. It means that MCSNet can effectively extract each subject's lower limb movement feature, thereby achieving good movement prediction.

2) Cross-Subject Classification: In the case of cross-subject, we randomly selected the data of three subjects to train the model and selected the data of two subjects as the validation set. The whole process is repeated ten times, producing ten different folds.

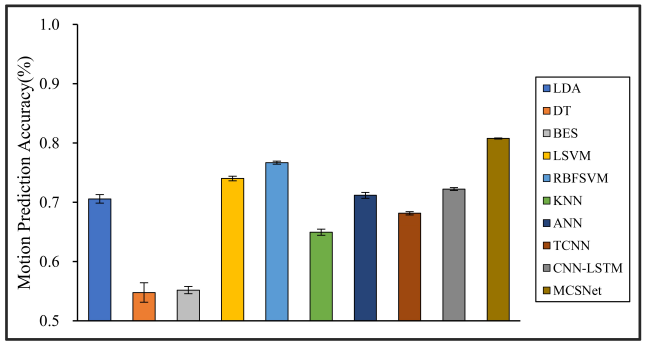

Fig. 5. Cross-subject movement prediction performance, averaged over all folds. Error bars denote two standard errors of the mean.

Cross-subject prediction results across all models are shown in fig. 5. It can be seen that the traditional and deep learning-based MHRI movement prediction models

have poor performance in the cross-subject situation, with an average accuracy rate of about 70%. However, the MCSNet model proposed in this paper can still achieve an accuracy of 80.25% in lower limb movement prediction, which has a significant statistical difference ($P < 0.05$). This result shows that the MCSNet model proposed in this paper can extract the deep common features of different subjects under the same lower limb movement. The model has good robustness.

IV. CONCLUSIONS

In this paper, a channel synergy-based human-exoskeleton interface is proposed for lower limb movement prediction in paraplegic patients. It uses the sEMG signals of 12 upper limb muscles as input signals, which can avoid the problem of weak sEMG signals in the lower limbs of paraplegic patients. The interface constructs a channel synergy-based network (MCSNet), it uses LSTM, depthwise and separable convolutions to extract the spatiotemporal features of multi-channel sEMG signals, and introduces an attention module to extract the synergy of different sEMG feature channels. An sEMG acquisition experiment is designed to verify the effectiveness of the MCSNet model. The results show that MCSNet has a good movement prediction performance in both within-subject and cross-subject situations. What's more, the movement prediction time of MCSNet is estimated. Plus the sEMG acquisition time (about 300 *ms*), the entire movement prediction time is about 400 *ms*, which is much shorter than the movement execution time of the exoskeleton. This means that MCSNet can be used on the actual lower limb exoskeletons. In the future, we consider applying the proposed human-exoskeleton interface to an actual exoskeleton platform. In addition, we will focus on multi-modal movement prediction based on sEMG and EEG.

ACKNOWLEDGMENT

This work was supported by the National Key Research and Development Program of China (No. 2018AAA0102504), the National Natural Science Foundation of China (NSFC) (No. 62003073), the Sichuan Science and Technology Program (No. 2021YFG0184, No. 2020YFSY0012, No. 2018GZDZX0037), and the Research Foundation of Sichuan Provincial Peoples Hospital (No. 2021LY12)

REFERENCES

[1] Simo M, Mendes N, Gibaru OandNeto P, "A Review on Electromyography Decoding and Pattern Recognition for Human-Machine Interaction," *IEEE Access*, 2019, 7: 39564-39582.

[2] Ding M, Nagashima M, Cho S-G, Takamatsu JandOgasawara T, "Control of Walking Assist Exoskeleton with Time-Delay Based on the Prediction of Plantar Force," *IEEE Access*, 2020, 8: 138642-138651.

[3] Zhu L, Wang Z, Ning Z, Zhang Y, Liu Y, Cao W, Wu XandChen C, "A Novel Motion Intention Recognition Approach for Soft Exoskeleton Via Imu," *Electronics*, 2020, 9(12).

[4] Beil J, Ehrenberger I, Scherer C, Mandery CandAsfour T, "Human Motion Classification Based on Multi-Modal Sensor Data for Lower Limb Exoskeletons," *Ieee Int Conf Intell Rob Syst*, 2018: 5431-5436.

[5] Ortiz M, Ianez E, Contreras-Vidal J LandAzorin J M, "Analysis of the Eeg Rhythms Based on the Empirical Mode Decomposition During Motor Imagery When Using a Lower-Limb Exoskeleton. A Case Study," *Front Neurorobot*, 2020, 14.

[6] Suplino L O, Sommer L F, Forner-Cordero AandIeee, "Emg-Based Control in a Test Platform for Exoskeleton with One Degree of Freedom," *Proc. Annu. Int. Conf. Ieee Eng. Med. Biol. Soc. Embs*, 2019: 5366-5369.

[7] Zhuang Y, Leng Y, Zhou J, Song R, Li LandSu S W, "Voluntary Control of an Ankle Joint Exoskeleton by Able-Bodied Individuals and Stroke Survivors Using Emg-Based Admittance Control Scheme," *IEEE Trans Biomed Eng*, 2021, 68(2): 695-705.

[8] Gu L, Yu Z, Ma T, Wang H, Li ZandFan H, "Eeg-Based Classification of Lower Limb Motor Imagery with Brain Network Analysis," *Neuroscience*, 2020, 436: 93-109.

[9] Wang C, Wu X, Wang ZandMa Y, "Implementation of a Brain-Computer Interface on a Lower-Limb Exoskeleton," *IEEE Access*, 2018, 6: 38524-38534.

[10] Tariq M, Trivailo P MandSimic M, "Eeg-Based Bci Control Schemes for Lower-Limb Assistive-Robots," *Front Hum Neurosci*, 2018, 12.

[11] Kawamoto H, Lee S, Kanbe S, Sankai YandIeee I, "Power Assist Method for Hal-3 Using Emg-Based Feedback Controller," *Ieee Trans. Syst. Man Cybern. Syst.*, 2003: 1648-1653.

[12] Wang C, Guo Z, Duan S, He B, Yuan YandWu X, "A Real-Time Stability Control Method through Semg Interface for Lower Extremity Rehabilitation Exoskeletons," *Front Neurosci*, 2021, 15(280).

[13] Villa-Parra A C, Delisle-Rodriguez D, Botelho T, Mayor J J V, Delis A L, Carelli R, Frizera Neto AandBastos T F, "Control of a Robotic Knee Exoskeleton for Assistance and Rehabilitation Based on Motion Intention from Semg," *Res Biomed Eng*, 2018, 34(3): 198-210.

[14] Hinton G, Deng L, Yu D, Dahl G E, Mohamed A-r, Jaitly N, Senior A, Vanhoucke V, Patrick N, Sainath T NandKingsbury B, "Deep Neural Networks for Acoustic Modeling in Speech Recognition," *IEEE Signal Process Mag*, 2012, 29(6): 82-97.

[15] LeCun Y, Bengio YandHinton G, "Deep Learning," *Nature*, 2015, 521(7553): 436-444.

[16] He K, Gkioxari G, Dollar P, Girshick RandIeee, "Mask R-Cnn," *Proc Ieee Int Conf Comput Vision*, 2017: 2980-2988.

[17] Huang G, Liu Z, van der Maaten L, Weinberger K QandIeee, "Densely Connected Convolutional Networks," *Proc Ieee Comput Soc Conf Comput Vision Pattern Recognit*, 2017: 2261-2269.

[18] Allard U C, Nougarou F, Fall C L, Giguere P, Gosselin C, Laviolette F, Gosselin BandIeee, "A Convolutional Neural Network for Robotic Arm Guidance Using Semg Based Frequency-Features," *Ieee Int Conf Intell Rob Syst*, 2016.

[19] Jabbari M, Khushaba R N, Nazarpour KandIeee, "Emg-Based Hand Gesture Classification with Long Short-Term Memory Deep Recurrent Neural Networks," *Proc. Annu. Int. Conf. Ieee Eng. Med. Biol. Soc. Embs*, 2020: 3302-3305.

[20] Cote-Allard U, Fall C L, Drouin A, Campeau-Lecours A, Gosselin C, Glette K, Laviolette FandGosselin B, "Deep Learning for Electromyographic Hand Gesture Signal Classification Using Transfer Learning," *IEEE Trans Neural Syst Rehabil Eng*, 2019, 27(4): 760-771.

[21] d'Avella A, Saltiel PandBizzi E, "Combinations of Muscle Synergies in the Construction of a Natural Motor Behavior," *Nat Neurosci*, 2003, 6(3): 300-308.

[22] d'Avella A, Portone A, Fernandez LandLacquaniti F, "Control of Fast-Reaching Movements by Muscle Synergy Combinations," *J Neurosci*, 2006, 26(30): 7791-7810.

[23] Phinyomark A, Phukpattaranont PandLimsakul C, "Feature Reduction and Selection for Emg Signal Classification," *Expert Syst Appl*, 2012, 39(8): 7420-7431.

[24] Englehart KandHudgins B, "A Robust, Real-Time Control Scheme for Multifunction Myoelectric Control," *IEEE Trans Biomed Eng*, 2003, 50(7): 848-854.

[25] Phinyomark A, Quaine F, Charbonnier S, Serviere C, Tarpin-Bernard FandLaurillau Y, "Emg Feature Evaluation for Improving Myoelectric Pattern Recognition Robustness," *Expert Syst Appl*, 2013, 40(12): 4832-4840.

[26] Clevert D, Unterthiner T, Hochreiter S, "Fast and Accurate Deep Network Learning by Exponential Linear Units (elus)," 2016: arXiv:1511.07289.

[27] Kingma D PandBa J, "Adam: A Method for Stochastic Optimization," 2014: arXiv:1412.6980.

[28] Ceseracciu E, Reggiani M, Sawacha Z, Sartori M, Spolaor F, Cobelli C, Pagello E, "SVM Classification of Locomotion Modes using Surface Electromyography for Applications in Rehabilitation Robotics," *Proc. IEEE Int. Workshop Robot Human Interact. Commun*, 2010.